Modeling land use changes and their impact on sediment load in a Mediterranean watershed

Romano Giovanni [1], Abdelwahab Ossama.M.M [2,1], Gentile Francesco[1].

[1] Department of Agricultural and Environmental sciences, University of Bari Aldo Moro, Bari, 70126, Italy.

[2] Department of Agricultural Engineering, Faculty of Agriculture, Cairo University, 12613, Giza, Egypt.

Corresponding Author:

Ossama.M.M. ABDELWAHAB

Department of Agricultural and Environmental sciences, University of Bari Aldo Moro

Bari, 70126, Italy.

E-mail: osama.mahmoud@agr.cu.edu.eg

Tel.: +39 080 54430592109

Modeling land use changes and their impact on sediment load in a Mediterranean watershed

Abstract

The aim of this study is to model potential changes in land use and evaluate their effects on sediment load in a Mediterranean watershed, the Carapelle, in Southern Italy. For this purpose, a set of Landsat Thematic Mapper (TM) images were processed to generate three different land use maps for 1987, 2002, and 2011. The images were corrected for geometric distortion and atmospheric interference before performing an unsupervised classification and decision expert system post classification. The land use maps for 1987 and 2002, derived from the Landsat TM processing, were analyzed using a Land Change Modeler (LCM) module to identify transitions from the first land cover type to the second. The transitions were modeled using a multi-layer perceptron (MLP) neural network to create transition potential maps, which provide the controls for subsequent dynamic land use change predictions. The model produced a predicted land use map for 2011 using Markov Chain analysis, which was validated with the actual 2011 land use map. Consequently, a land use scenario (S1) for 2035 and 2050 was predicted, taking into account the current constraints and management options. LCM was further used to define two additional scenarios (S2 and S3) both for 2035 and 2050 based on different land management options.

Finally, the Annual Agricultural Non-Point Source Pollution Model (AnnAGNPS) was used to estimate the effect of the predicted land use changes on sediment load after model calibration, using a five-year dataset registered at the Ordona monitoring station.

The land use change analysis revealed low transformations from 1987 to 2011. Equally, land use changes were low for the base scenario (S1) so moderate variations in sediment load were estimated. The changes in land use were more significant for the additional scenarios (S2 and S3) and consequently the model estimations underwent major variations, with a significant reduction of soil erosion. The associated utilization of land use change analysis and AnnAGNPS modeling

demonstrates how land use management options can be adopted to reduce potential watershed sediment load.

Key Words: Land use change; Remote sensing; GIS; Sediment load; AnnAGNPS model

1. Introduction

Land use and land cover (LULC) change is a complex process that can affect erosion and sediment load rates in a watershed (Abdelwahab et al., 2014). Climate and several human activities are capable of exacerbating LULC change (Pelacani el al., 2008; Leh et al., 2013) and the dynamics of erosive processes. Severe alterations of LULC, due to increases or decreases in human population and response of the population to economic opportunities (Lambin et al., 2001; Chung et al., 2011), have numerous consequences for terrestrial and aquatic environments (Wilson and Weng, 2011). For this reason, the understanding of recent land use changes and how these changes will occur in the future is of fundamental importance (Rounsevell et al., 2006). This knowledge is crucial for decision support procedures to identify appropriate land use policies (Romano et al., 2015), and for decision makers, environmentalists and planners in the development of plans to tackle environmental issues (Theobald and Hobbs, 2002; Maestas et al., 2003).

Many studies have been performed on the impact of land use changes on hydrology, water quality, and erosion at the watershed scale (Jeppesen et al., 2009; Tu, 2009; Feng et al., 2010; Alatorre et al., 2012; Wang et al., 2016). These studies found that the hydrological cycle and erosion processes are closely connected to land cover changes. Other studies focused on the impact of urbanization on hydrology (De Fries and Eshleman, 2004; White and Greer, 2006; Cuo, 2016), reporting that an increase of human settlements causes a decrease in infiltration and an increase in runoff. Fewer studies have addressed the combined effect of land use and climate changes on hydrology and surface water quality, as well as on erosion (Asselman et al., 2003; Chang, 2004; Li et al., 2009; Tu, 2009). Some of these works present responses that are simplified or not fully understood at the sub-watershed scale

(Wilson and Weng, 2011). Other studies focused on the impact of landuse changes on runoff and sediment connectivity at a watershed scale (López-Vicente et al., 2013; Lizaga et al., 2017; Persichillo et al., 2018).

An increasing number of studies have highlighted the importance of remote sensing multi-temporal imagery in understanding landscape dynamics (e.g., Rawat and Kumar, 2015). Remote sensing data, processed using geographic information system (GIS) software, have proven to be a very useful tool in land use studies, especially to detect, map, and model land cover patterns occurring in a given area over a determined period of time (Kahya et al., 2010; Rawat and Kumar, 2015). The integration of remote sensing with specific GIS supported hydrological models can substantially assist not only the investigation of land use changes, but also the influence of these changes on soil degradation and river system quality.

Many studies (Lopez et al., 2001; Petit et al., 2001; Rounsevell et al., 2006) have focused on predicting future land use composition, however, only a few have combined this analysis with hydrological models to predict potential water quality and soil erosion impacts (Chung et al., 2011; Praskievicz and Chang, 2011; Leh et al., 2013). For this purpose, a large number of hydrological models are available, such as the Soil and Water Assessment Tool (SWAT) (Arnold 1998), ArcView Generalized Watershed Loading Functions (AVGWLF) (Evans and Lehning, 2001), Hydrological Simulation Program—Fortran (HSPF) (Bicknell et al., 1996), and Annualized Agricultural Non-Point Source Pollution (AnnAGNPS) (Bingner et al., 2012). AnnAGNPS, in particular, was developed to evaluate the impacts of agricultural non-point source pollution on water quality (Bingner et al., 2012).

In this study, we investigated the impact of LULC changes on sediment load in the Carapelle watershed (Northern Puglia, Italy) with the combined use of satellite remote sensing, GIS, and hydrological modeling. Given the extension of the Carapelle watershed (506 km^2) and the complexity of its land cover distribution, remote sensing was considered to be an essential tool for the extensive study of land cover patterns in a realistic time frame at reasonable cost. Furthermore, the integration with GIS provides a useful tool for data analysis, update, and retrieval (Chilar, 2000). The specific objectives of the study are to:

- analyze historical and actual land use maps, starting with the preprocessing of Landsat 5 TM images up until their classification and expert post classification;
- identify and validate the trend of land cover change (with the help of a change analysis module), and predict a possible future scenario of land use (base scenario, S1), for years 2035 and 2050;
- individuate two additional land use scenarios (S2 and S3), both for years 2035 and 2050, based on different management options, developed according to directives dictated by the European Planning and European Agricultural Fund for Rural Development (EAFRD);
- evaluate the impacts of these predicted land use scenarios on sediment load at the watershed and sub-watershed scale.

2. Material and methods

2.1. Study area

The study was conducted in the Carapelle watershed, located in Northern Puglia, Southern Italy, and mouthed at the monitoring station of Ordona bridge (Fig. 1). The Carapelle torrent crosses Northern Puglia and parts of the Campania region. The torrent furrows the Daunia Mountains and, after crossing the Tavoliere Floodplain, flows into the Adriatic Sea. The hydrological regime is torrential as flood events are associated with intense and short-term rainfalls (Bisantino et al., 2010). The sediment transport is characterized by fine suspended materials and occurs mainly during the flood events (Gentile et al., 2010). The climate is typical Mediterranean with warm, dry summers and mild, moist winters; the average yearly rainfalls range from 450 to 800 mm y^{-1}, and the average monthly temperatures range from 10 to 16 °C (Trombetta et al., 2016).

The watershed area is 506 km^2. Altitudes range between 120 and 1075 m a. s. l., while the average slope is 8.2%. The mountainous areas of the watershed are subjected to considerable erosion, as shown by the high rates of suspended sediment transport during flood events (García-Rama et al., 2016). They are constituted by flysch formations, while the alluvial plain is characterized by clay-sand Plio-Pleistocene sediments (Abdelwahab et al., 2016b). Soils in the area mainly belong to the Entisols class with a fine clay-loam texture; the organic matter content is low and the fertility is prevalently natural. The plain and low hilly areas are mainly used for wheat cultivation and, to a lesser degree, olive orchards and agricultural crops, while deciduous oaks and hardwoods (*Quercus pubescens* s.l. and *Quercus cerris* L.) cover the higher slopes together with coniferous, pasture, and meadow (Aquilino et al., 2014). The area occupied by each land use and its percentage compared to the total watershed area is reported in Tab. 1. A monitoring station that provides water discharge and suspended sediment transport data is located at the watershed outlet (Gentile et al., 2008).

The study area has a very low population density (49 inhabitants per km^2). Eight municipalities fall within the watershed boundary, the most populated is Ascoli Satriano, with 6204 inhabitants, while Rocchetta Sant'Antonio is the least populated, with 1843 inhabitants (source: ISTAT, 2017). The entire territory has a predominant agricultural vocation. Cereal cultivation (winter wheat) is the main agricultural resource, and actually this trend is stopped from the first half of the nineteenth century, which led to a continuous deforestation (Massafra and Salvemini, 2005). Trade is scarcely developed throughout the area; the mining activity is limited to a site close to the outlet at Ordona bridge. Even if several dams have been built on watercourses in northern Puglia (one on the Fortore, seven on the Ofanto and one on the Celone), there are no dams along the Carapelle. A decreasing trend of annual rainfall was observed in the area from 1921 to 2001. This trend is mainly due to a series of scarce annual rainfalls from about 1980, with the 1988–1992 and 2000–2001 periods as the driest (Polemio and Casarano, 2008).

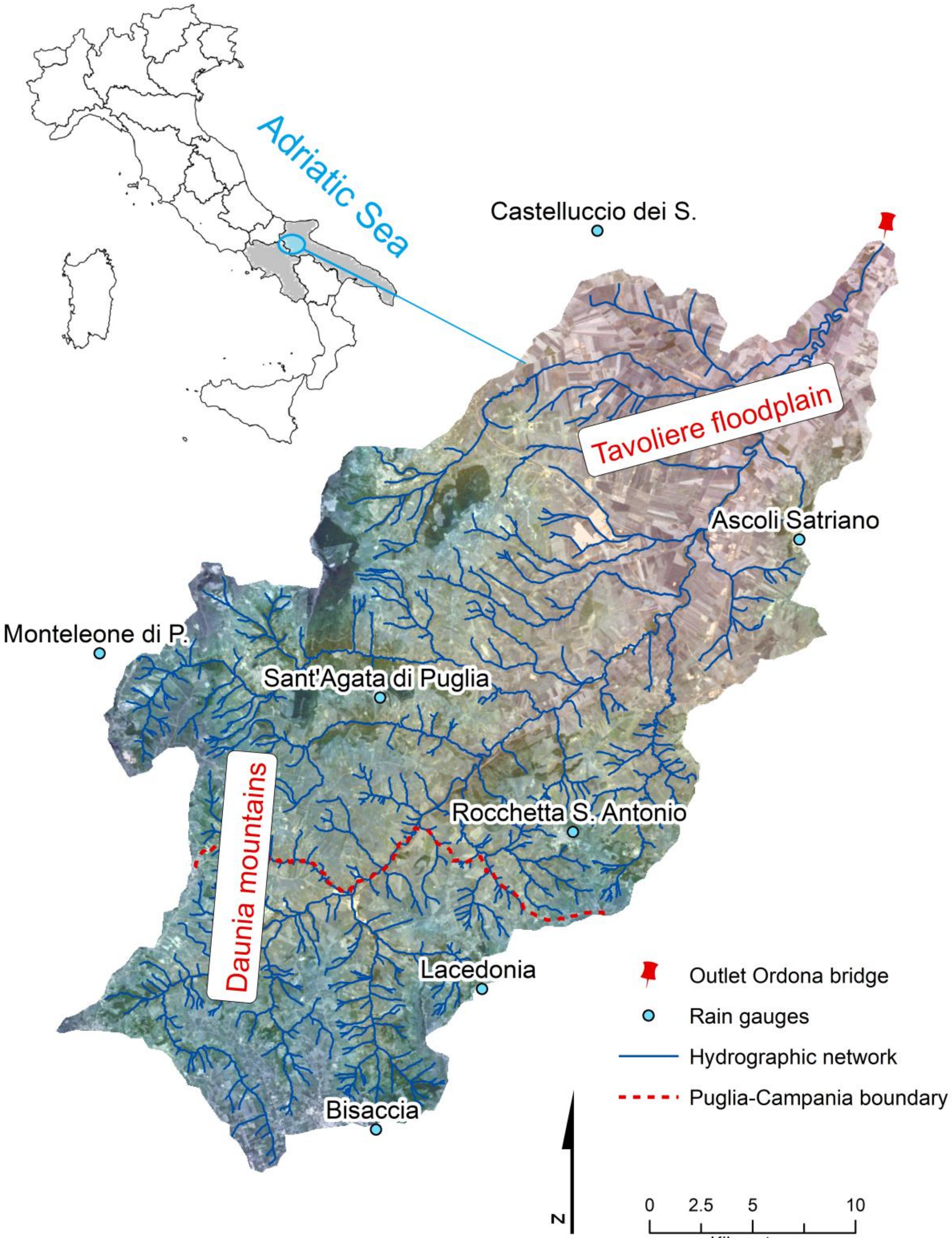

Fig. 1 – The Carapelle watershed mouthed at the Ordona bridge monitoring station.

2.2. Landsat images processing

The Landsat 5 TM images were chosen for their appropriate spatial resolution and for being the longest continuous record of image data observations available. The Landsat TM data and imagery provided by the later series of Landsat sensors (MSS, ETM, ETM+, OLI) have been extensively used for land cover analyses since the start of the Landsat program in 1972 (Kahya et al., 2010; Sexton et al., 2013). The TM sensor images are available in six reflective bands with a spatial resolution of 30 m and thermal band of 120 m.

The images used in this study were acquired by Landsat TM sensors on May 19, 1987, June 22, 2002, and June 22, 2011, and downloaded using the EarthExplorer Get Data tool (http://earthexplorer.usgs.gov) of the U.S. Geological Survey (USGS) Landsat web page. The images were chosen from those taken during the spring season, before the crop harvest, and with complete lack of cloud cover in order to meet the observation requirements revealing both natural and human-induced land cover changes.

Each TM scene was corrected for geometric distortion using the TerrSet cubic convolution resampling type with an RMS of about 0.2 pixels. Radiance corrections for atmospheric interference were performed using the Chavez Cos(t) model. These corrections improved the comparison capacity between images taken from different acquisition dates, as in the case study, and/or by different Landsat sensors. The Cos(t) model incorporates all elements of the dark object subtraction method (Jensen, 2005) for haze removal, as well as a procedure for estimating the effects of absorption by atmospheric gases and Rayleigh scattering.

The input for the atmospheric correction consists of raw image data that represent, for L1 products, the radiance captured by the TM sensor as reflected solar energy, and rescaled into a 8-bit digital number (Dn) that ranges between 0 and 255. Conversion from Dn back to a t-sensor spectral radiance (L_λ) requires a set of calibration parameters such as acquisition date and time, sun elevation, wavelength of band center, Dn haze, and the radiance value at Dn zero and Dn max (Lmin and Lmax, respectively). Alternatively, two band-specific rescaling factors, such as the slope (gain) and intercept (bias) of the TM sensor instrumental regression, can be used (Chander et al., 2009). The output in each case is an image of proportional reflectance that is expressed as a real number value between 0.0 and 1.0. Most of the data necessary for a full accommodation of the model are available on the metadata file associated with the downloaded imagery.

A hybrid approach was used to classify the Landsat TM images. In an early stage, an iterative self-organizing data analysis (ISODATA) classifier was implemented because the classification accuracy obtained from per-pixel supervised methods did not allow an univocal identification of the main types of land uses in the area. The reason for the low accuracy indices can be attributed to the difficulty in exactly determining the several land cover types for the fragmented territorial patches in the Carapelle watershed. Lastly, a decision expert post-classification was performed.

A set of aerial ortho-photos, displayed as a Web Map Service (WMS) from the Portale Cartografico Nazionale (PCN) (www.pcn.minambiente.it) or Portale Cartografico Regione Puglia (http://www.sit.puglia.it/), and the Corine Land Cover (CLC) maps were employed to assess the accuracy of the TM image classifications. The request response includes one or more georeferenced map images that can be displayed or queried in a browser application or GIS environment. CLC maps and reports are available for download from the Copernicus Land Monitoring Service (http://land.copernicus.eu/pan-european/corine-land-cover) and European Environment Agency (http://www.eea.europa.eu/publications/COR0-landcover).

The GIS used for remote sensing elaborations and prediction of the future land use changes was TerrSet (Clark Labs, 2015), developed by Clark University, USA. The computer simulation model used to predict the most likely future land use configuration of the studied area was based on potential transition techniques instead of regression models, which, despite application simplicity, require a considerable amount of data. The transition potential modeling framework is based on the stochastic Markov chain technique (Wu et al., 2006).

2.3. LULC change analysis and future land use prediction

The Land Change Modeler (LCM), a TerrSet application oriented to land conversion (Clark Labs, 2015), was used to perform a LULC change analysis between the 1987, 2002 and 2011 land uses. In a preliminary step, the LCM Change Analysis routine provided a set of tools for the analysis of gains and losses in land use classes, land cover persistence, and transitions between categories for the input map layers of 1987, 2002 and 2011. A total of 44 transitions took place between 2002 and 2011. According to their frequency distribution, transitions smaller than 8 ha were ignored and a total of 11 transitions were considered in the prediction runs.

A double stage approach was employed in developing future land use configurations. The classified land use maps for 1987 and 2002 were used as observed data for the calibration of the LCM Transition Potentials module. The LCM Change Prediction function was then employed to simulate the land use map for 2011, whereas the classified land use map for 2011 (Obs_11) served to verify the accuracy of the simulated map in the validation stage.

In order to derive the transition potential of each land cover class, a collection of environmental variables that potentially contributed to land use change was tested by exploring both their potential explanatory power and association strength. A set of six static and one dynamic explanatory variables were selected for the LCM transition potential modeling routine. Other environmental variables were excluded for their low potential power.

The static variables (e.g., drivers that remained unchanged over the simulation period), which encompass elevation, distances between natural and anthropic settlements (e.g., streams, roads and urban) and slope, evidence the likelihood of land cover class changes between 2002 and 2011. Evidence likelihood is an empirical probability of change for a qualitative map and is not primarily represented with numeric values. The dynamic variable is the distance from the areas where a transition from a land use class to another one takes place. It is a time-dependent driver that is recalculated at specific intervals during the prediction period (Eastman, 2006). Explanatory variables and the strength of their association with the distribution of land cover categories were defined by computing the Cramer's *V* statistic (Ott et al., 1983). A multi-layer perceptron (MLP) neural network was then used to model each transition potential, which resulted in a transition potential map for each of the LULC changes.

The MLP dynamic process was performed with 4 + 4 classes, one hidden layer, a dynamic learning rate, a momentum factor of 0.5, and 10,000 iterations. This created a random sample of pixels that experienced each modeled transition, and an additional set of random samples for the persistent cases. Based on the explanatory variables value at a given location, the neural network process developed a multivariate function to predict the transition potential by using half of the samples to train the model and the other half to test it. A consistent accuracy rate higher than 80 %and an equally high skill measure were obtained between the training and testing datasets. Because of the high accuracy values and sequential cross-tabulation results between observed and simulated maps for 2011, it was not deemed appropriate to modify the default MLP parameters.

The model transition potentials were utilized in the LCM Change Prediction module to develop the simulated land use map for 2011 in order to validate a comparison with the observed data, and then to predict future land cover maps for 2035 and 2050.

Based on the real trend of the land use changes that have been occurred between 2002 and 2011, the model predicted a first scenario (S1) for 2035 and 2050. In scenario S1, all land use classes had their normal parameterization. The factors with few chances to improve the forecasting process and/or that are hardly integrable with the biophysical factors, were neglected (Verburg et al., 2004).

Scenario S1 was developed using the Markov chain analysis, which is a random-stochastic process that undergoes transitions from one state to another within a fixed time. The probability of the transition to the next state, according to Markov theory, depends exclusively on the current state features and not on the preceding sequence of events (Gamermann, 1997; Häggström, 2002; Kocabas and Dragicevic, 2006).

LCM provides two models of change: 1) a soft prediction model which maps the areas that are likely to be transformed and yields a map of vulnerability to change for each land use class; 2) a hard prediction model, based on a competitive land allocation similar to a multi-objective decision process (Clark Labs, 2015), which maps only the selection of areas with the higher suitability to change and yields a single realization map.

Two additional scenarios (S2 and S3) were performed, for the same years 2035 and 2050, taking into account incentives and constraints arising from socio-economic drivers. In scenario S2, incentives were given for the abandonment of cereal cultivation. This scenario reflects the agronomic regime (set-aside) introduced by European Union (EU) in 1988 (Regulation (EEC) 1272/88) (http://eur-lex.europa.eu/legal-content/en/ALL/?uri=CELEX:31988R1272) with the aim of reducing cereal cultivation and controlling the price reduction of agricultural products. Afterwards it was focused on the environmental implications of the set-aside, considered an effective practice to improve biodiversity on arable farmland, especially on a period of five years (Hester and Harrison, 2007). The set-aside is still in use in the Carapelle watershed, although as a practice for crop rotation or for meeting the current UE incentives.

The S2 scenario was defined for cereal cultivation areas with a slope greater than 20%, distance from urban settlements greater than 8 km, and distance from primary roads greater than 3 km, in order to minimize income reduction due to the modified cropping system. In the fields where cereal is no longer cultivated, natural grass vegetation grows and with time becomes pastureland with the presence of shrubs typical of Mediterranean maquis (Pignatti, 1995). Such agronomic practice was implemented for the years 2035 and 2050 (S2_35 and S2_50 scenarios) in order to evaluate its effects on the sediment load in the watershed.

In scenario S3, the incentives given in scenario S2 for the abandonment of cereal cultivation are replaced with incentives for substituting cereals with deciduous forests. In this scenario, the development of a 150 m wide riparian buffer along the main stream is also added in order to take into account one of the major goals of the current European Agricultural Fund for Rural Development (EAFRD) (http://eur-lex.europa.eu/legal-content/EN/TXT/PDF/?uri=CELEX:32013R1305&from=IT) regarding restoring, preserving, and enhancing ecosystems related to agriculture and forestry. This scenario was also implemented for the years 2035 and 2050 (S3_35 and S3_50 scenarios).

2.4. AnnAGNPS model description

The AnnAGNPS model (Theurer and Cronshey, 1998; Bingner and Theurer, 2005; U.S. Department of Agriculture (USDA)-Agricultural Research Service (ARS), 2006) is a distributed-parameter model based originally on the single-event model AGNPS (Young et al., 1989). The USDA-ARS and Natural Resources Conservation Service (NRCS) developed the original AGNPS and AnnAGNPS to evaluate sediment and chemical delivery from an un-gauged agricultural watershed up to 3000 km^2 (Bosch et al., 2001; Abdelwahab et al., 2014). The model is a continuous simulation, batch-process computer program where the watershed is divided into many homogeneous (with respect to soil type, land use, and land management) drainage areas (cells), connected to each other by a network of channels and reaches. Runoff volume, sediment, and nutrient and pesticide rates are routed from their origins in upland drainage areas through the defined channel network to the watershed outlet (Bingner and Theurer, 2005; Abdelwahab et al., 2013).

The input data required by the AnnAGNPS model are of two major types: a daily climate record and a description of the physical characteristics and management of the watershed. The climatic data requirements for simulations include daily precipitation, maximum and minimum air temperatures, average daily dew point temperature, wind direction and speed, and sky cover or solar radiation. The second type of input data comprises morphological parameters, agricultural practices, and crops and soil data. The hydrologic runs of the model are based on a simple water balance approach that includes interception, evaporation, surface runoff, evapotranspiration, subsurface lateral flow, and subsurface drainage (Yuan et al., 2006). The Soil Conservation Service (SCS) curve number (CN) technique (USDA, 1972) is used to determine surface runoff and peak flow rate, while the revised universal soil loss equation (RUSLE) (Renard et al., 1997) is used to predict sheet and rill erosion. The sediment delivery ratios of total sediment are determined using the hydro-geomorphic universal soil loss equation model (Theurer and Clarke, 1991). Sediment transport in streams is computed using a modified Einstein equation, and the sediment transport flow capacity is estimated using the Bagnold (1966) equation (Bingner and Theurer, 2005). Lastly, soil moisture balance is calculated on a sub-daily time step using a simple constant-time step procedure (Abdelwahab et al., 2016).

2.5. AnnAGNPS model data setup

Topographic characteristics of the watershed were identified using a 20-m resolution digital elevation model (DEM), provided by the Shuttle Radar Topographic Mission carried out by NASA and NGA. The watershed topographic evaluation and watershed parameterization were performed using the topographic parameterization program (TOPAZ). A subset of TOPAZ, TOPAGNPS, includes TOPAZ modules used for AGNPS. TOPAGNPS processes a raster DEM to: identify and measure topographic features; define surface drainage, flow direction, and flow paths; subdivide watersheds along drainage divides into sub-watersheds; quantify the drainage network; calculate channel parameters; and estimate representative sub-watershed parameters (Garbrecht and Martz, 1995). By setting the critical source area (i.e., minimum drainage area below which a permanent channel is defined) and minimum source channel length to 50 ha and 250 m, respectively, 1177 sub-watersheds (cells) and 477 streams (reaches) were generated. This watershed delineation achieved the best spatial description of the watershed because it counts all soil physical, topographical, and management characteristics and, at the same time, leads to a reasonable amount of computation.

Soil characteristics were extracted from the agro-ecological characterization of the Puglia region project named ACLA2 (scale 1:100,000), which is aimed at the agro-ecological characterization of the region based on field observations, laboratory tests, and the interpretation of aerial photos and satellite images (Caliandro et al., 2005). The soil types in the watershed have different texture classes with approximately 90% of the total watershed area composed of loam, silty clay loam, and sandy clay loam soils (Milella et al., 2012). The soil hydraulic properties (i.e., water content at wilting point, field capacity, and saturated hydraulic conductivity) were obtained using the pedotransfer functions of Saxton and Rawls (2006).

The RUSLE factors LS and C were internally calculated by the model as functions of topography and management, whereas the R factor was calculated after Ferro and Porto (2000). Data from eight rain gauges located in the watershed and its surroundings included in the Puglia civil protection agency network were used to identify the rainfall distribution in the watershed. The average annual rainfall ranges from 553 mm in 2007 to 871 mm in 2010, with an average annual value of 670 mm. Rainfall is intense between September and April, with March being the rainiest month (average annual value = 92 mm) while August is the driest (average annual value = 6 mm). The SCS synthetic hyetograph Type I, which best describes Mediterranean conditions (Bisantino et al., 2015), was considered during simulation to represent the rainfall distribution in the watershed (USDA_NRCS, 1986). Other climate input data, including minimum and maximum temperatures, dew point, wind speed, and solar radiation, were obtained from the Puglia civil protection agency.

The winter wheat crop parameters were derived from the AnnAGNPS model's associated RUSLE database, whereas the management practices applied in the watershed were carefully identified through field surveys and farmer interviews. A four-year crop rotation is typically adopted in the watershed, where winter wheat is cultivated for three years followed by a forage crop (e.g. red clover). Winter wheat is typically sowed in November and harvested in July. Discharge records and sediment transport data, used for the AnnAGNPS model calibration, were provided by a monitoring station located at the watershed outlet (Gentile et al., 2008).

Visual examination and statistical indices were used to assess the model performance. The most common statistical index was R^2, whose drawback is the tendency to mask even very poor fittings.. The Nash and Sutcliffe efficiency (NSE) (1970) is based on the ratio of the residual variance to the data variance. This value estimates the extent to which a plot of simulated values against observed data approximates a 1:1 line. The percent bias (PBIAS) assesses how much the model over- or underestimates the data.

3. Results and discussion

3.1. Landsat images classification and model validation

Following the unsatisfactory results of the supervised classification, as reported in section 2.2, a hard classification of the TM data was performed for all spectral bands, except thermal band 6. In a later stage, the results of the hard classifier were used in post-classification by a decision expert system. Eleven land use classes (Table 1) were produced after cross-tabulation with the CLC maps followed by a patch-by-patch comparison with the PCN aerial ortho-photos.

The accuracy of the classified maps was checked on a pixel basis using a stratified random sampling method and 70 samples were selected for each land cover category. The data collected from the classified land cover maps were compared with the reference data corresponding to the real land use conditions. Image classification accuracies ranged between 90% and 92%, and exceeded the minimum threshold established for remotely sensed images reported by Congalton (1991).

Table 1 – Land use land cover area measurements for 1987, 2002, and 2011.

Categories	1987		2002		2011		Δ 1987-2011	
	km^2	%	km^2	%	km^2	%	km^2	%
Urban and rural residential	5.76	1.15	7.48	1.49	9.53	1.90	3.78	65.60
Highway	1.31	0.26	1.30	0.26	1.30	0.26	-0.01	-1.03
Water	3.54	0.70	3.51	0.70	3.55	0.71	0.01	0.31
Coniferous forest	3.83	0.76	3.87	0.77	3.88	0.77	0.05	1.22
Deciduous forest	28.25	5.62	29.07	5.79	29.43	5.86	1.19	4.20
Mixed forest	5.92	1.18	5.74	1.14	5.74	1.14	-0.18	-3.10
Mediterranean maquis/Shrubs	18.33	3.65	17.61	3.51	16.59	3.30	-1.74	-9.47
Meadow/Pasture/Fallow	22.23	4.42	17.75	3.53	15.42	3.07	-6.81	-30.63
Olive	10.22	2.03	10.36	2.06	10.21	2.03	0.00	-0.03
Cereal cultivation	392.25	78.07	395.79	78.77	396.63	78.94	4.38	1.12

Agricultural crop	10.83	2.15	9.99	1.99	10.17	2.02	-0.65	-6.04

The precision of the simulated map was assessed visually with the LCM validation module, and quantitatively by performing a cross-tabulation with the real 2011 land use data map. The results of the confusion matrix point out an overall accuracy of about 0.93 and a Kappa Index of Agreement (KIA) of about 0.97. The user's accuracy ranged between 0.778 and 0.9977 (with the exclusion of the highway land use class), whereas the producer's accuracy ranged between 0.8237 and 1 (Table 2).

Table 2 – Accuracy indices obtained after cross-tabulation between classified (Obs_11) and projected 2011 land use maps.

Categories	KIA	User's accuracy	Producer's accuracy
Urban and rural residential	0.7742	0.7780	0.8691
Highway	0.9993	0.9993	1.0000
Water	0.9872	0.9873	0.9995
Coniferous forest	0.9977	0.9977	1.0000
Deciduous forest	0.9776	0.9789	0.9759
Mixed forest	0.9876	0.9878	0.9997
Mediterranean maquis/Shrubs	0.9127	0.9157	0.8874
Meadow/Pasture/Fallow	0.8245	0.8298	0.8237
Olive	0.9802	0.9806	0.9572
Cereal cultivation	0.9396	0.9874	0.9853
Agricultural crop	0.8993	0.9002	0.9675

The obtained KIA values (Table 2), according to Pontius and Millones (2011), show an almost perfect agreement (KIA>0.8) for all classes, except for the urban areas (substantial agreement) where transformations were likely less correlated to the biophysical variables selected but might require the incorporation of socio-economic and political drivers. The results show an acceptable performance of the land use prediction model.

3.2. LULC change analysis between 1987 and 2011

Land cover classification maps for the Carapelle watershed were produced for each of the years 1987, 2002 and 2011. For each land use class and for the three observation years, surface area values (Table 1) and losses/gains (Fig. 2a) were detected using LULC change analysis. The results show that urban and rural residential areas and cereal cultivation increased respectively by 3.78 km^2 and 4.38 km^2 from 1987 to 2011; Mediterranean maquis decreased by 1.74 km^2, while meadow, pasture and fallow decreased by 6.81 km^2. Urban areas grew steadily from 1987 to 2002 and from 2002 to 2011, whereas cereal cultivation experienced an increase mainly from 1987 to 2002. Large transformations in the other land use typologies were not observed, except for a moderate deciduous forest increase , corresponding to 1.19 km^2, mostly from 1987 to 2002 (Table 1).

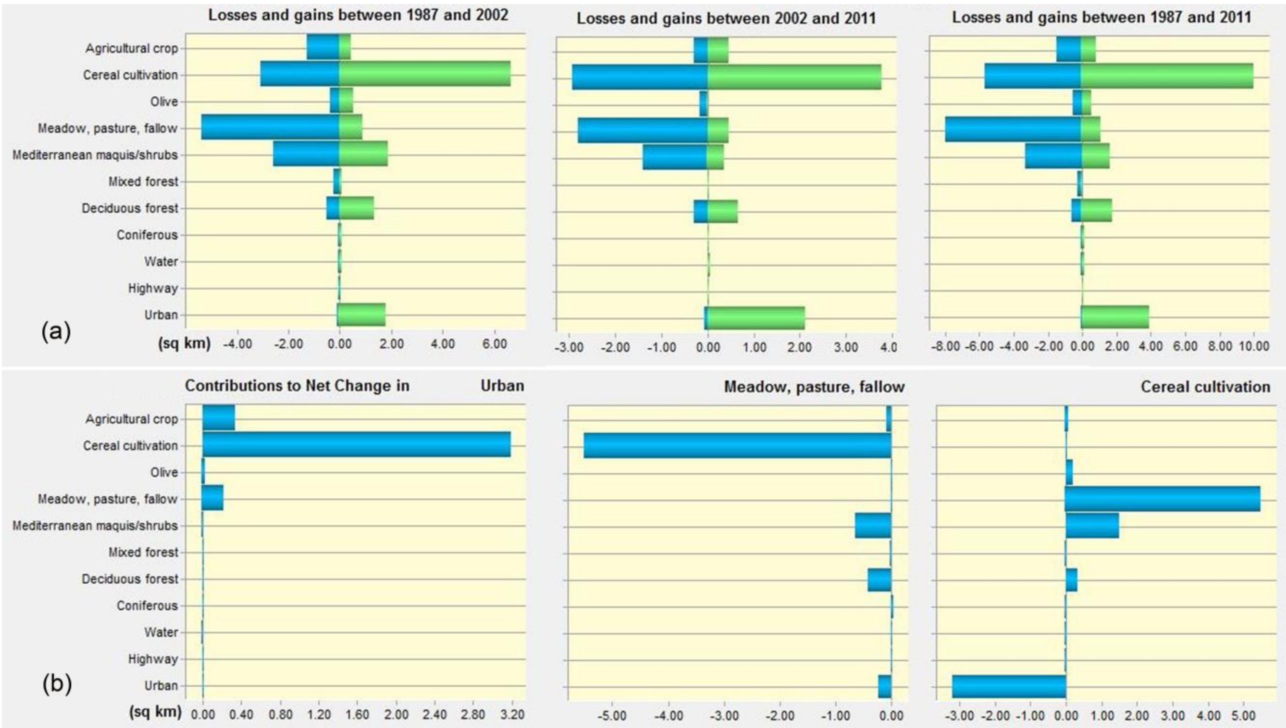

Fig. 2 – (a) LULC losses and gains between 1987, 2002, 2011; (b) Contributions to net change in urban; meadow, pasture, fallow; cereal cultivation.

The proportion of urban areas increased mainly at the expense of cereal, agricultural, and pasture areas, with the highest contribution from cereal crops (3.19 km^2), as showed by Fig. 2b. The reduction in meadows/pasture area was lost at the favor of cereal, Mediterranean maquis, and deciduous forest areas, with the highest contribution for cereal areas (5.50 km^2). Although cereal cover decreased by more than 3 km^2 for urban areas, this accounted for only 0.64% of the watershed area and its surface increased between 1987 and 2011 by contributions from meadows, maquis (1.49 km^2) and deciduous forest (0.32 km^2).

A careful analysis of the data revealed a lack of a well identifiable trend for the period. The agricultural vocation of the territory seems unchanged and does not demonstrate the impact of planning tools aimed at developing any of the land use type in the area or of some new types. Hence, the observed fragmentation in the territory land use and associated changes are mainly related to individual activities.

3.3. Predicted LULC change analysis

Land use in the S1 scenario estimates surface variations for the watershed land use classes, both in 2035 and 2050 (Table 3). The S2_35 and S3_35 scenarios show that the size of land use classes involved by the socio-economic incentives (e.g., cereal cultivation and meadow/pasture/fallow for S2, cereal cultivation and deciduous forest for S3) change consistently (Table 3). Cereal cultivation decreases, in both S2_35 and S3_35, by 23.05 and 25.59 % respectively in relation to the 2011 spatial extent, whereas meadow/pasture/fallow and deciduous forest areas increase their surface proportion in S2 by 23.32 % and a very slight reduction (0.98 %) in S3 (Table 3). Other land use classes also show slight surface variations in S2 and S3.

Land use change analysis between 2011 and 2050 confirms the same trend previously predicted for 2035 (Table 3). With the exception of slight countertrends among some land use classes, spatial gains and losses simulated for 2050 appear slightly higher than the respective values indicated for 2035.

The land use maps for S1_35 and S1_50 show significant development of urban areas where all land use classes had normal parameterization without incentives and constraints (Fig. 3 and Fig.

4). Pronounced development of meadow is observed in the cereal cultivation lands in S2, and the development of deciduous forest along the riparian areas and in the cereal cultivation lands in S3, as imposed by the respective incentives (Fig. 3 and Fig. 4). Cereal cultivation is the dominant land use in scenario S1 with a very slight reduction in area in 2035 and 2050. For the other two scenarios, areas occupied by cereal cultivation were reduced in the S2_35 and S3_35 scenarios, as previously reported, and by 22.78 % and 25.32 % for the S2_50 and S3_50 scenarios, respectively.

Table 3 – Land use areas in 2011, and predicted land use percent change (Δ) of the different scenarios (S1, S2, S3) through the periods (2011-2035) and (2011-2050)

Categories	2011	**Δ 2011-2035**			**Δ 2011-2050**		
		S1	**S2**	**S3**	**S1**	**S2**	**S3**
Urban and rural residential	1.90	1.05	**-**	**-**	**1.69**	**-**	**-**
Highway	0.26	-	**-**	**-**	**-**	**-**	**-**
Water	0.71	-	**-**	**-**	**-**	**-**	**-**
Coniferous forest	0.77	-	**-**	**-**	**-**	**-**	**-**
Deciduous forest	5.86	0.19	**0.19**	**27.55**	**0.28**	**0.28**	**27.92**
Mixed forest	1.14	-	**-**	**-0.003**	**-**	**-**	**-0.003**
Mediterranean maquis/Shrubs	3.30	-0.50	**-0.50**	**-0.77**	**-0.76**	**-0.76**	**-1.04**
Meadow/Pasture/Fallow	3.07	-0.92	**23.32**	**-0.98**	**-1.30**	**23.21**	**-1.34**
Olive	2.03	-0.05	**-0.05**	**-0.15**	**-0.09**	**-0.09**	**-0.19**
Cereal cultivation	78.94	0.13	**-23.05**	**-25.59**	**0.04**	**-22.78**	**-25.32**
Agricultural crop	2.02	0.10	**0.10**	**-0.05**	**0.15**	**0.15**	**-0.03**

Scenario S1: the land use maps in 2035 and 2050 were predicted based on the real trend of the land use changes during the observation period (2002-2011).

Scenario S2: the land use maps in 2035 and 2050 were predicted taking into account incentives for the abandonment of cereal cultivation in the marginal areas (set-aside).

Scenario S3: the land use maps in 2035 and 2050 were predicted taking into account incentives for replacing cereal cultivation, in the marginal areas, with deciduous forests and the development of a 150 m wide riparian buffer along the main stream.

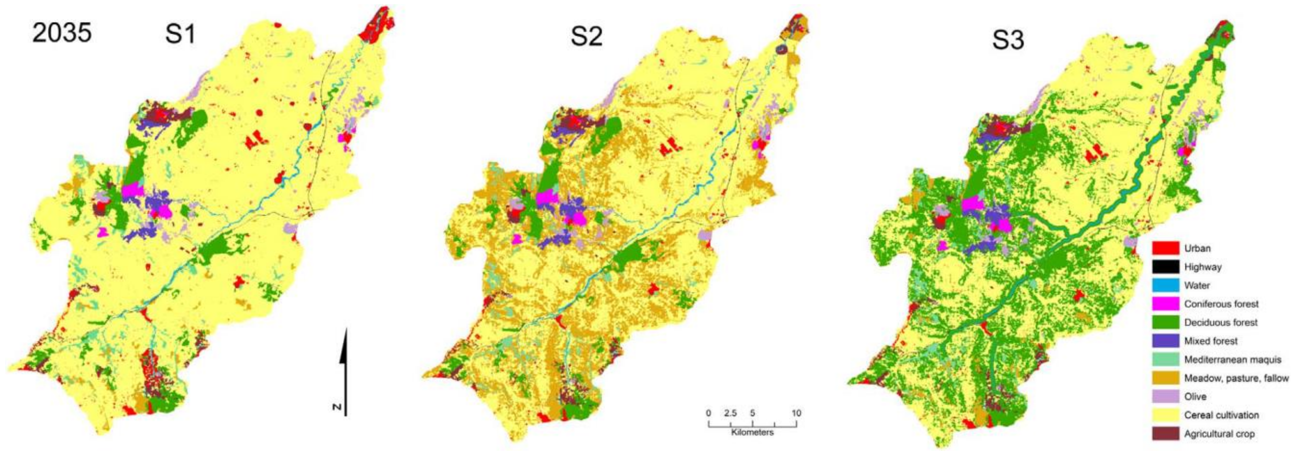

Fig. 3 – Carapelle watershed land use maps for scenarios S1, S2, and S3 in 2035.

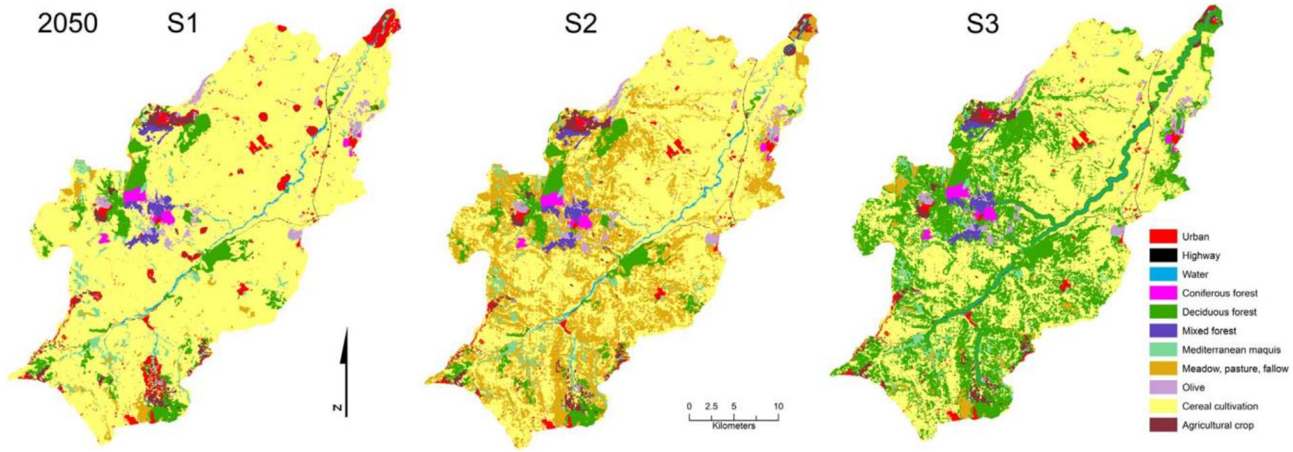

Fig. 4 – Carapelle watershed land use maps for scenarios S1, S2, and S3 in 2050.

3.4. AnnAGNPS calibration

3.4.1 Runoff

The accumulated totals for observed runoff and sediment load for each simulation year through the period 2007–2011 were compared with their corresponding simulated values. The main objective when calibrating the model was to constrain the sediment component in order to study the impact of the land use change on soil erosion. As it is well known that the hydrological component of the model is the driving factor for all model simulations, this component was calibrated first. Many studies that used AnnAGNPS (Yuan et al., 2001; Baginska et al., 2003; Shrestha et al., 2006; Licciardello et al., 2007; Polyakov et al., 2007; Das et al., 2008; Parajuli et al., 2009; Taguas et al., 2009; Bisantino et al., 2015) reported CN as the most sensitive input parameter for surface runoff prediction. Before calibration, the initial CN were set for each land use category as proposed by the SCS (1986).

On an annual scale, the model had a tendency to underestimate runoff before calibration (31% less than observed runoff). In order to improve the match between the observed and simulated runoff, CN values were increased (+10, +5, +2%) for each land use category. AnnAGNPS was run several times using the modified CN values each time and the statistical analysis was then recalculated. The best simulated values were obtained when CN values were increased by 2% of the initial values, showing a total runoff quantity of 167 mm $year^{-1}$, which was nearly 6% less than the observed value (177 mm $year^{-1}$). These results are in agreement with a study by Shamshad et al. (2008) in Malaysia where statistical analysis showed that the runoff volume produced good results (R^2 = 0.92, E = 0.85) when CN values were increased by 2%. The statistical indices show good model estimation for runoff. In general, the positive PBIAS value of 15.17 shows a slight runoff underestimation on the annual scale.

The simulated and observed runoff were also compared on a monthly scale. According to Moriasi et al. (2007), the statistical indices demonstrated satisfactory model performance in estimating runoff, while the PBIAS value (15.17) showed a model runoff underestimation. The comparison between observed and simulated runoff on a monthly scale is shown in Fig. 5 where it can be seen that AnnAGNPS under-predicts runoff for every month except for September, October, November, and December. In light of the fact that in July, August, September, and October, fields are not covered by winter wheat and that tillage operations were applied, the underestimation could be explained with the model sensitivity to the cover crop conditions (Yuan et al., 2001). Chahor et al. (2013) used the AnnAGNPS model to simulate runoff and sediment loads in a smaller Mediterranean agricultural watershed (207 ha) located in the region of Navarre (Spain) and showed that the model satisfactorily simulated surface runoff with calibration at monthly and annual scales (NSE = 0.75, 0.63 and R^2 = 0.79, 0.78, respectively).

3.4.2 Sediment load

Default model runs showed a tendency to overestimate sediment load before calibration. To optimize sediment estimation, a calibration was carried out by adjusting the RUSLE-P factor. Renard et al. (1997) reported that the RUSLE-P factor can have a value between 0.4 and 0.6 in watershed conditions under different slope percentages. The best results were obtained for P = 0.5. The Manning coefficient was also increased for cropland and rangeland by 50% in order to reduce the sediment overestimation. After calibration, sediment load prediction was improved at an annual scale. The average annual amounts were 6.1 Mg ha^{-1} y^{-1} and 5.8 Mg ha^{-1} y^{-1} for simulated and measured sediment load, respectively, corresponding to a 4% difference. Statistical indices show satisfactory model performance on an annual time scale (R^2 = 0.61, NSE = 0.41, PBIAS = -0.02).

On a monthly scale, the highest sediment loads were concentrated during November, December, January, March, and April because of intensive rainfall events occurring during those months (Fig. 5). The model capability of estimating sediment load on a monthly basis (Fig. 5) showed satisfactory results (R^2 = 0.65, NSE = 0.52, PBIAS = -0.02) according to Moriasi et al. (2007). This finding is in agreement with a study by Taguas et al. (2009), in which sediment at the monthly scale also showed satisfactory values (NSE = 0.6, R^2 = 0.8). Chahor et al. (2013) calibrated the AnnAGNPS model for sediment load simulation. The model was capable of simulating the sediment load at an annual scale with a difference of less than 1% for calibration and 7% for validation. However, comparison between predicted and observed sediment loads on a monthly and seasonal basis showed unsatisfactory results (NSE = 0.13, R^2 = 0.2).

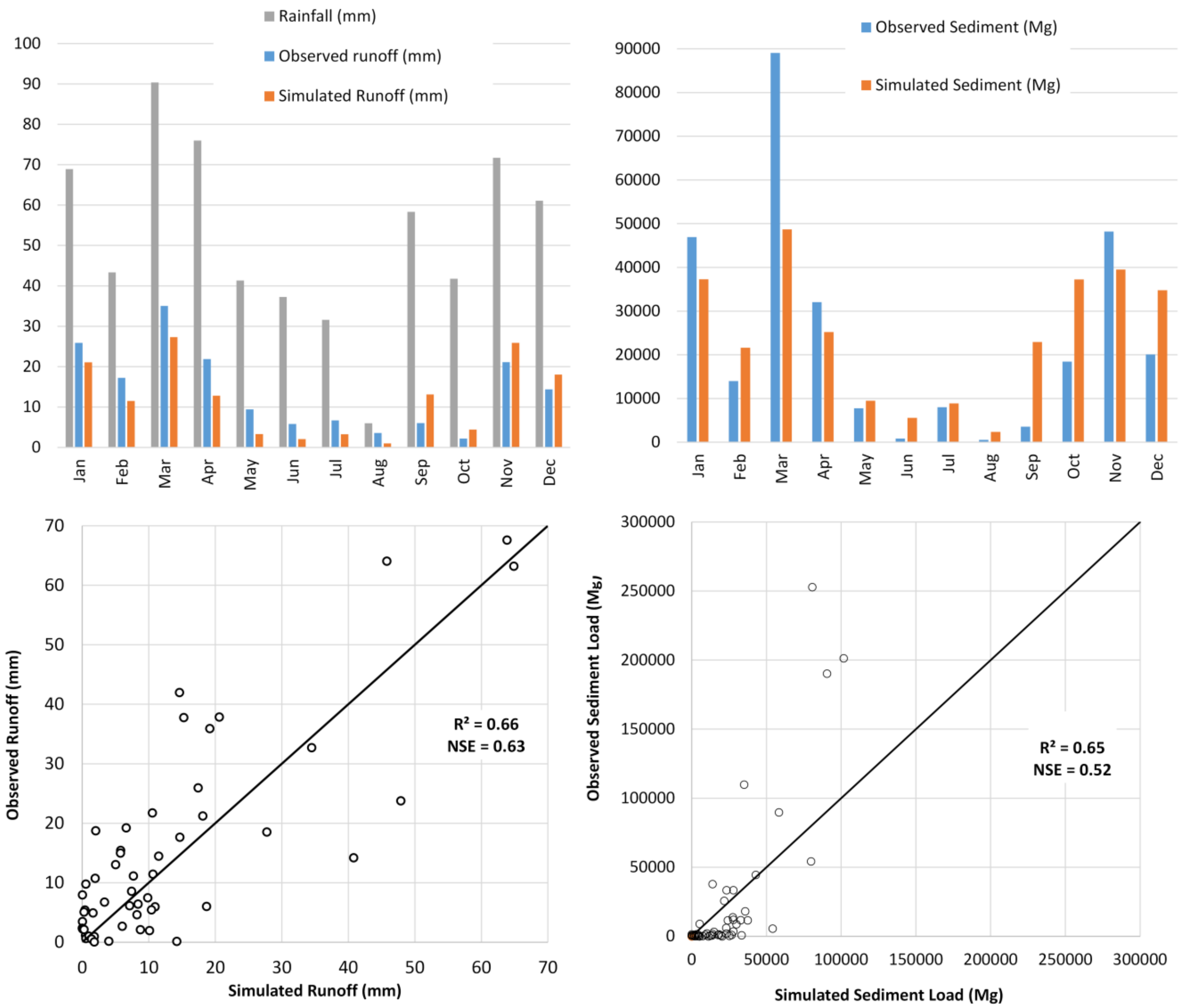

Fig. 5 – Monthly observed and simulated Runoff and sediment loads.

3.5. Future land use scenarios and their impact on sediment load

The AnnAGNPS model was used to study the impact on sediment load of three future scenarios (S1, S2, S3) for each year (2035, 2050) to be compared with the observed land use in 2011 (Obs_11). The average annual runoff was calculated for each scenario. Scenarios S1_35 and S1_50 achieved a very slight change in runoff, in which scenario S1_35 showed an increase by 0.3% and S1_50 showed a decline by -0.2%. Scenarios S3_35, S3_50, and S2_35 showed almost similar results as runoff was reduced by approximately 18.8%, 18.9%, and 19.1%, respectively. For sediment load at the watershed outlet, the results show that the average annual sediment loads increased by 0.3% and 0.1% in scenarios S1_35 and S1_50, respectively.

The remaining four scenarios showed an average annual sediment reduction that ranged from 21.9% to 23.6%. The highest reduction was seen in the cases of S3_50 and S3_35 with reductions by 23.6% and 23.4%, respectively. The sediment load was reduced to 4.63 Mg ha^{-1} y^{-1} in scenario S3_50 compared with 6.07 Mg ha^{-1} y^{-1} in Obs_11. The three scenarios for the year 2035 show a strong similarity with those for 2050. This fact could be due to the very slight change in the land use configuration from 1987 to 2011, which in turn has affected the land change model prediction of future scenarios. This stability in the land use configuration of the watershed was also seen in 2035 and 2050, which did not lead to substantial influence on the hydrological or sediment component of the AnnAGNPS model.

The AnnAGNPS results were used to evaluate soil erosion rates at the sub-watershed scale under different land use configurations predicted by LCM. The soil erosion values estimated for the 2011 and 2050 scenarios were reclassified into five classes based on the degree of severity (Fig. 6). As expected, erosion rates were not subject to large variations from the Obs_11 to S1_50 scenarios. The mean value observed is 5.34 Mg ha^{-1} y^{-1} for 2011, and 5.24 Mg ha^{-1} y^{-1}, for S1_50. In both cases, the maximum erosive value is about 21.47 Mg ha^{-1} y^{-1}.

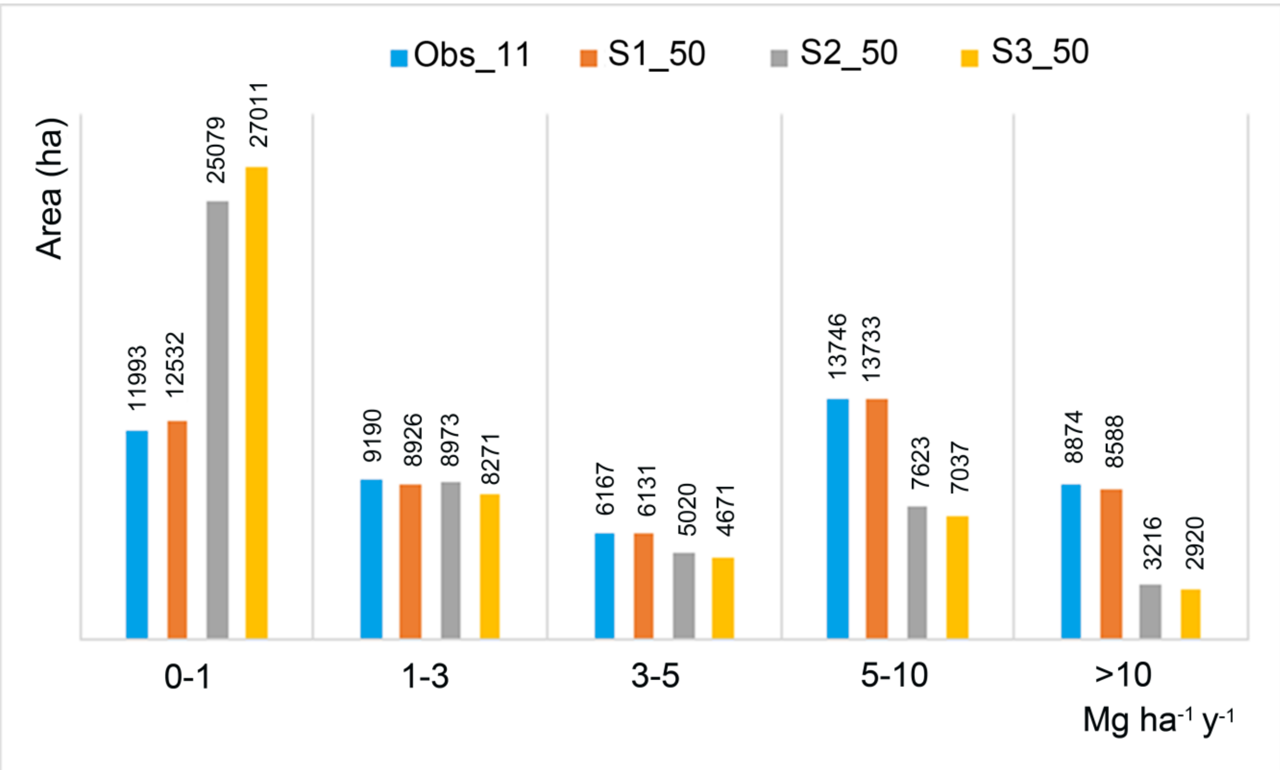

Fig. 6 – Soil erosion classes for Obs_11 and S1_50, S2_50, and S3_50 scenarios.

Significant variations were observed for the S2_50 and S3_50 scenarios. For these two scenarios, the soil erosion class distributions show a significant reduction of the mean soil erosion values (2.75 Mg ha^{-1} y^{-1} and 2.52 Mg ha^{-1} y^{-1}, respectively) due to a sharp increase in the lower classes, as well as a decreasing distribution from zero to highest values, with a maximum observed erosive value of about 16.54 Mg ha^{-1} y^{-1}. The average estimated soil erosion for S3_50 is slightly lower than S2_50 (-0.23 Mg ha^{-1} y^{-1}), which is likely due to the fact that deciduous forest protects soil better than pasture and that in S3_50, there is a wooded area along the buffer zone of the main stream. It is believed that the difference between the soil erosion estimated for S3_50 and that for S2_50 is quite small because the pasture in the latter scenario provides sufficient soil protection. Furthermore, the action of deciduous forest in the buffer zone is low since it replaces the cereal cultivation mostly in flat areas rather than in areas with higher slopes.

Scenarios S2_50 and S3_50 show a substantial reduction of the sites with high erosion rates compared with Obs_11 and S1_50. Such a territorial context favors the planning of management practices that affect a lower number of sediment source areas. Consequently, the effectiveness of erosion control intervention may be optimized by targeting fewer risky erosion sites.

The S1_50 class with the lowest erosion (from 0 to 1 Mg ha^{-1} y^{-1}) experiences an areal increase of 5.02%, compared with the same erosion class of Obs_11. For S2_50 and S3_50, the increase was 110.14% and 126.35%, respectively. In the other classes (1–3, 3–5, 5–10, >10 Mg ha^{-1} y^{-1}), a reduction of area was observed from 2011 to 2050 for all scenarios considered. In the 1–3 Mg ha^{-1} y^{-1} class, the area reduction was low, less than 10% for S3_50, which is the scenario that demonstrates the greatest reduction for this class. The reduction was about 24.3% in the third class (3–5 Mg ha^{-1} y^{-1}) for the S3_50 scenario. The area reduction was more significant for the last two classes (5–10 and >10 Mg ha^{-1} y^{-1}). In the first case (5–10 Mg ha^{-1} y^{-1}), percentages range from 0.1% in S1_50 to 44.55%

in S2_50, and up to 48.41% in S3_50. The reduction percentage was even more accentuated for the last class (>10 Mg ha^{-1} y^{-1}), which reached 67.10% for S3_50.

It is interesting to compare the spatial distribution of different erosion classes for scenarios S1_50 and S3_50, as shown in Fig. 7. The substitution of cereal cultivation in the marginal areas of the watershed with deciduous forest results in a reduction of the higher erosion classes (5–10 and >10 Mg ha^{-1} y^{-1}) in scenario S3_50, especially in the mountainous areas with higher slopes. In particular if we consider the watershed areas with an altitude greater than 500 m a.s.l. and a slope greater than 10%, the surface occupied by the two higher erosion classes (5–10 and >10 Mg ha^{-1} y^{-1}) is 131.29 km^2 in scenario S1_50 and 51.47 km^2 in scenario S3_50; if we consider only the highest erosion class (>10 Mg ha^{-1} y^{-1}) the surface is 65.32 km^2 in scenario S1_50 and 21.32 km^2 in scenario S3_50).

This suggests that a widespread use of deciduous forest on high slope areas would be an appropriate management practice in such territorial context.

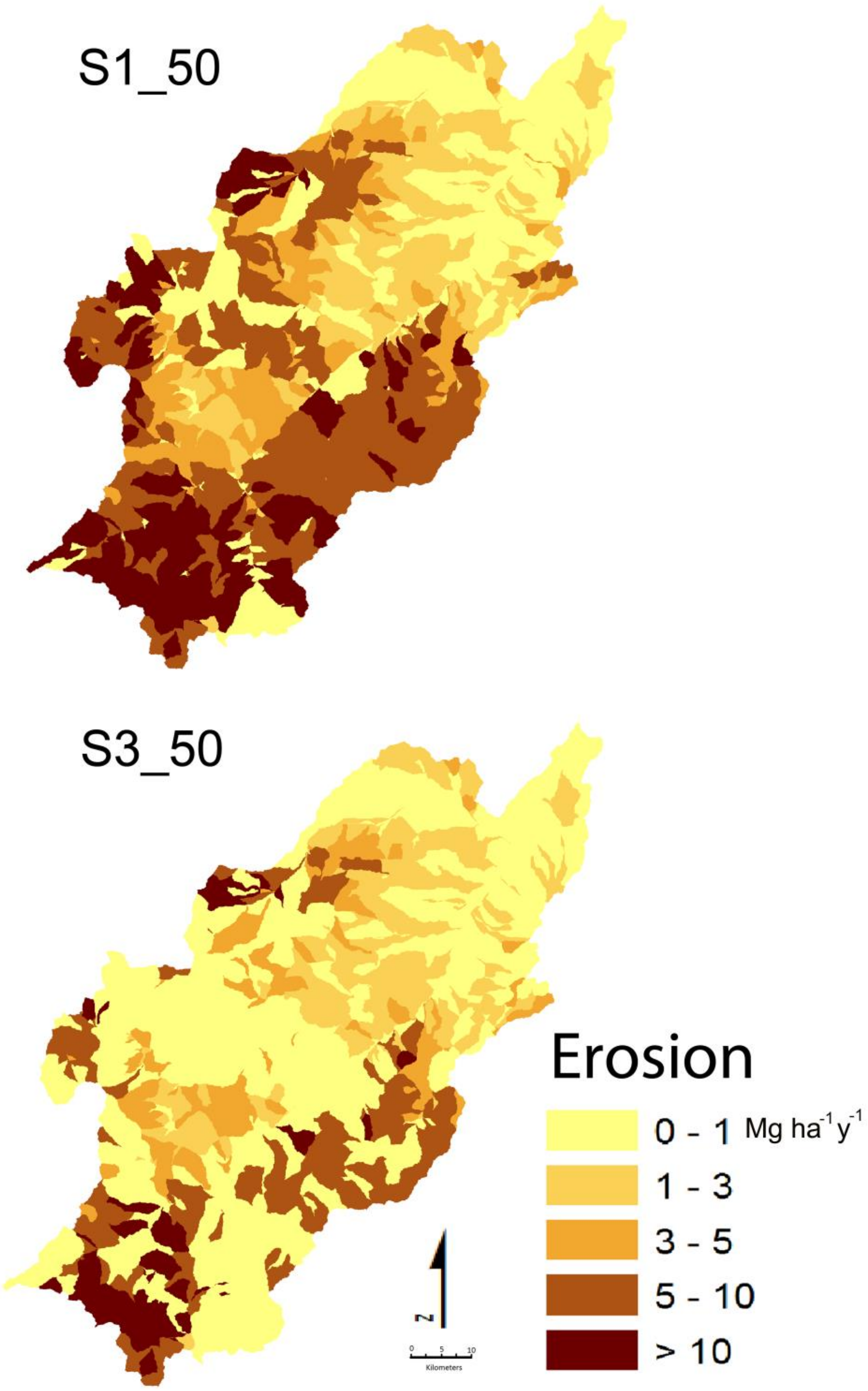

Fig. 7 – Predicted erosion potential map for S1_50 and S3_50 scenario

Conclusions

The aim of this study is to identify the potential effects of land use changes on spatial distribution and entity of soil erosion in the Carapelle watershed. A long-term land use analysis performed from 1987 to 2011 using Landsat imagery and LCM, reveals the poor propensity of the area to experience large changes in the studied period. This trend is confirmed considering the predicted land use in 2035 and 2050 (scenario S1), based on a Markov's chain analysis. Two additional land use scenarios (S2 and S3) were then developed, including in the LULC analysis two different management options of the watershed, which are based on the regional socio-economic trends and EAFRD guidelines.

Taking into account the results of the land use analysis, the AnnAGNPS distributed model was used to investigate the rate and distribution of soil erosion in the watershed. The high erosion rates estimated in 2011 were not subject to significant variations in the S1 scenario. In this scenario, soil erosion reaches high levels (>10 Mg ha^{-1} y^{-1}) in many sites, which can cause a considerable degree of loss in soil fertility. Significant positive variations were conversely observed for the S2 and S3 scenarios since a relevant reduction I n the sediment load was estimated. Even if both management options were useful in reducing the higher rates and areal distribution of soil erosion in the watershed, in scenario S2 the replacement of winter wheat with fallow responds exclusively to political and economic directives. Scenario S3, conversely, has a more complex effect, as the replacement of winter wheat with deciduous forest and riparian buffers generates also positive effects for the environment since it allows the development of more complex vegetation series with higher biodiversity.

The results obtained highlight the importance of modeling the impact of future land use changes on soil erosion. This is especially true in cases, like this Mediterranean agricultural watershed, where the erosion rates are actually high and the integrated use of land use change analysis and erosion modeling confirms this trend in the future. The methods described here are applicable by researchers and planners to identify which management options can be adopted to reduce soil erosion risk in such fragile environments, taking into account the distribution of soil erosion at a watershed scale as well as environmental, political and economic constraints.

Acknowledgements

This work was carried out in the framework of the Project "Soil erosion in Puglia: monitoring, modeling and control strategies", funded by Puglia Watershed Authority, Coordinator prof. Francesco Gentile (University of Bari "A. Moro", Italy).

References

Abdelwahab, O.M.M., Bisantino, T., Milillo, F., Gentile, F., 2013. Runoff and sediment yield modeling in a medium-size Mediterranean watershed. *Journal of Agricultural Engineering*, 44, art. no. e7, 31-40.

Abdelwahab O.M.M., Bingner R.L., Milillo F., Gentile F., 2014. Effectiveness of Alternative Management Scenarios on the Sediment Load in a Mediterranean Agricultural Watershed. *Journal of Agricultural Engineering*, Vol. 45, No 3.

Abdelwahab, O.M.M., Bingner, R.L., Milillo, F., Gentile, F., 2016a. Evaluation of Alternative Management Practices with the AnnAGNPS Model in the Carapelle Watershed. *Soil Science*, 181 (7), 293-305.

Abdelwahab, O.M.M., Milillo, F., Gentile, F., 2016b. Modeling soil erosion and sediment load at different time scales in a medium-sized watershed. *2016 American Society of Agricultural and Biological Engineers Annual International Meeting*, ASABE 2016.

Aquilino, M., Novelli, A., Tarantino, E., Iacobellis, V., Gentile, F., 2014. Evaluating the potential of GeoEye data in retrieving LAI at watershed scale. *Proceedings of SPIE - The International Society for Optical Engineering*, 9239, art. no. 92392B.

Alatorre L.C., Begueria S., Lana-Renault N., Navas A., Garcia-Ruiz J.M., 2012. Soil erosion and sediment delivery in a mountain catchment under scenarios of land use change using a spatially distributed numerical model. *Hydrol. Earth Syst. Sci.*, 16, 1321-1334.

Asselman N.E., Middelkoop H., P.M. Dijk P.M., 2003. The impacts of changes in climate and land use on soil erosion, transportation and deposition of suspended sediment in the River Rhine. *Hydrol Processes*, 17, 3225–3244.

Baginska, B., Milne-Home, W., Cornish, P.S., 2003. Modelling nutrient transport in Currency Creek, NSW with AnnAGNPS and PEST. *Environmental Modelling and Software* 18, 801–808.

Bagnold R.A., 1966. An approach to the sediment transport problem from general physics. Prof. Paper 422-*J. U.S. Geol*. Surv., Reston, VA, USA.

Bicknell B. R., Imhoff J. C., Kittle J. L., Donigian A. S., Johanson R.C., 1996. Hydrological Simulation Program - FORTRAN User's Manual for Release 11. Environmental Research Laboratory, Office of Research and Development, U.S. Environmental Protection Agency, Athens, GA.

Bingner R.L., Theurer F.D., 2005. AnnAGNPS technical processes documentation, version 3.2. USDA-ARS National Sedimentation Laboratory, Oxford, MS, USA.

Bingner RL, Theurer FD. 2012. AGNPS Web Site, http://www.ars.usda.gov/Research/docs.htm?docid=5199

Bisantino, T., Gentile, F., Milella, P., Trisorio Liuzzi, G., 2010. Effect of time scale on the performance of different sediment transport formulas in a semiarid region. *Journal of Hydraulic Engineering*, 136 (1), art. no. 003001QHY, 56-61.

Bisantino, T., Bingner, R., Chouaib, W., Gentile, F., Trisorio, Liuzzi G., 2015. Estimation of runoff, peak discharge and sediment load at the event scale in a medium-size Mediterranean watershed using the AnnAGNPS model. *Land Degrad. Dev*. 26 (4), 340–355. http://dx.doi.org/10.1002/ldr.2213.

Bosch D., Theurer F., Binger R., Felton G., Chaubey I. 2001. Evaluation of the AnnAGNPS water quality model. In: J.L. Parsons, D.L. Thomas, and R.L. Huffman (eds.), Agricultural non-point source models: their use and application. Southern Cooperative Series Bulletin 398. http://s1004.okstate.edu/S1004/Regional-Bulletins/Modeling-bulletin/modeling-bulletin.pdf Accessed: March 2012.

Caliandro A., Lamaddalena N., Stellati M., Steduto P., 2005. Caratterizzazione agroecologica della Regione Puglia in funzione della potenzialità produttiva: Progetto Acla 2. Bari, Italy.

Chander G., Markham B.L., Helder D.L., 2009. Summary of current radiometric calibration coefficients for Landsat MSS, TM, ETM+, and EO-1 ALI sensors. *Remote Sensing of Environment, 113, 893-903.*

Chavez P.S., 1996. Image-Based Atmospheric Corrections – Revisited and Improved. *Photogrammetric Engineering and Remote Sensing*, 62, 9, 1025-1036.

Chang, H., 2004. Water quality impacts of climate and land use changes in Southeastern Pennsylvania. *The Professional Geographer*, 56, 240–257.

Chilar J., 2000. Land cover mapping of large areas from satellites: status and research priorities *Inter. J. Rem. Sen*., 21, 1093–1114

Chung E., Park K., Lee K.S., 2011.The relative impacts of climate change and urbanization on the hydrologic response of a Korean urban watershed. *Hydrol Processes*, 25, pp. 544–560.

Clark Labs, 2015. Clark University. 950 Main Street, Worcester MA 01610-1477, USA. Web: http://www.clarklabs.org

Congalton R.G.A., 1991. A review of assessing the accuracy of classification of remotely sensed data. *Remote Sens Environ*, 37, 35–46.

Copernicus Land Monitoring Service. http://land.copernicus.eu/pan-european/corine-land-cover

Cuo L.,2016. Land use/cover change impacts on hydrology in large river basins: a review. Terrestrial Water Cycle and Climate Change: Natural and Human-Induced Impacts 221: 103.

Das, S., Rudra, R.P., Gharabaghi, B., Gebremeske, S., Goel, P.K., Dickinson, W.T., 2008. Applicability of AnnAGNPS for Ontario conditions. *Canadian Biosystems Engineering* 50 (1), 1–11.

De Fries R., Eshleman K.N., 2004. Land-use change and hydrologic processes: a major focus for the future. *Hydrol. Process*., 18, 2183–2186.

Eastman J.R., 2006. Idrisi Andes Guide to GIS and Image Processing. Clark University, Worcester, M.A.

European Environment Agency. http://www.eea.europa.eu/publications/COR0-landcover

Evans B. M., Lehning, D. 2001. ArcView generalized watershed loading function, University Park, PA: Environmental Resources Research Institute. (Version 3.2).

Feng X., Wanga Y., Chen L., Fu B., Bai G., 2010. Modeling soil erosion and its response to land-use change in hilly catchments of the Chinese Loess Plateau. *Geomorphology*, 118, 3-4, 239-248.

Ferro, V., Porto, P., 2000. Sediment Delivery Distributed (SEDD) Model. *Journal of Hydrologic Engineering*, 5(4), 411-422. doi: 10.1061/(asce)1084-0699(2000)5:4(411)

Gamerman D., 1997. Markov Chain Monte Carlo: Stochastic Simulation for Bayesian Inference. Boca Raton, FL: CRC Press.

Garbrecht J., Martz L.W., 1995. TOPAZ: An automated digital landscape analysis tool for topographic evaluation, drainage identification, watershed segmentation and sub catchment parameterization: TOPAZ user manual. USDA-ARS Publication No. NAWQL 95-3. U.S. Department of Agriculture-Agricultural Research Service, Washington, DC, USA.

García-Rama, A., Pagano, S.G., Gentile, F., Lenzi, M.A., 2016. Suspended sediment transport analysis in two Italian instrumented catchments. Journal of Mountain Science, 13 (6), 957-970. doi: 10.1007/s11629-016-3858-x

Gentile, F., Bisantino, T., Corbino, R., Milillo, F., Romano, G., Trisorio Liuzzi, G., 2008. Sediment transport monitoring in a Northern Puglia watershed. WIT Transactions on Engineering Sciences, 60, 153-161. doi: 10.2495/DEB080161

Gentile F., Bisantino T., Corbino R., Milillo F., Romano G., Trisorio Liuzzi G., 2010. Monitoring and analysis of suspended sediment transport dynamics in the Carapelle torrent (Southern Italy). *Catena*, 80, 1–8.

Häggström O., 2002. Finite Markov Chains and Algorithmic Applications. Cambridge University press.

Hester R.E., Harrison R.M., 2007. Biodiversity Under Threat, ROC Publishing.

Jensen J.R., 2005. Introductory digital image processing: a remote sensing perspective. (3 rd edition) Upper Saddle River, NJ.

Jeppesen E., Kronvang B., Meerhoff M., Sondergaard M., Hansen K., Anderson H., 2009. Climate change effects on runoff, catchment phosphorus loading and lake ecological state, and potential adaptations. *J Environ Qual*, 38 (5), 1930–1941.

Kahya O., Bayram B., Reis S., 2010. Land cover classification with an expert system approach using landsat ETM imagery: a case study of Trabzon. *Environ Monit Assess*, 160, 431-438.

Keen-Zebert A., 2007. Channel responses to urbanization: Scull and Mud Creeks in Fayetteville, AR. *Physical Geography*, 28: 249-260.

Kocabas V, Dragicevic S. 2006. Coupling Bayesian networks with GISbased cellular automata for modeling land use change. *Geographic Information Science*, 4197, 217–233.

ISTAT, 2017. http://dati-censimentopopolazione.istat.it/

Lambin EF, Turner BL, Geist HJ, Agbola SB, Angelsen A, Bruce JW, Coomes OT, Dirzo R, Fischer G, Folke C, George PS, Homewood K, Imbernon J, Leemans R, Li X, Moran EF, Mortimore M, Ramakrishnan PS, Richards JF, Skånes H, Steffen W, Stone GD, Svedin U, Veldkamp TA, Vogel C, Xu J. 2001. The causes of land-use and land-cover change: Moving beyond the myths. *Global Environmental Change*, 11, 261–269. DOI: 10.1016/S0959-3780(01)00007-3

Leh M., Bajwa S., Chaubey I., 2013. Impact of land use change on erosion risk: an integrated remote sensing, geographic information system and modelling methodology. *Land Degradation & Development*, 24, 409-421.

Li Z., Liu W., Zhang X., Zheng F., 2009. Impacts of land use change and climate variability on hydrology in an agricultural catchment on the Loess Plateau of China. *Journal of Hydrology*, 377, 35–42.

Licciardello, F., Zema, D.A., Zimbone, S.M., Bingner, R.L., 2007. Runoff and soil ero-sion evaluation by the AnnAGNPS model in a small Mediterranean watershed. *Transactions of the ASABE* 50 (5), 1585–1593.Ministerio de Agricultura, Pesca y Alimentación, Dpto. de Agricultura, Ganaderíay Montes del Gobierno de Navarra, 1986. Caracterización agroclimática deNavarra. Dirección General de la Producción Agraria, Madrid. Instituto Navarrodel suelo, Pamplona.

Lizaga I., Quijano L., Palazón L., Gaspar L., and Navas A., 2017. Enhancing Connectivity Index to Assess the Effects of Land Use Changes in a Mediterranean Catchment. *Land Degrad. Develop*., doi: 10.1002/ldr.2676.

Lopez E., Bocco G.,Mendoza M., Duhau E., 2001. Predicting land cover and land use change in the urban fringe: a case in Morelia city, Mexico. *Landscape Urban Plann*, 55 (4), 271-285.

López-Vicente M., Poesen J., Navas A., Gaspar L., 2013. Predicting runoff and sediment connectivity and soil erosion by water for different land use scenarios in the Spanish Pre-Pyrenees. CATENA, Scales in Soil Erosion 102, 62-73. doi:10.1016/j.catena.2011.01.001

Maestas J.D., Knight R.L., Gilgert W.C., 2003. Biodiversity across a rural land-use gradient. *Conserv Biol*, 17 (5), 1425–1434.

Massafra A., Salvemini B., 2005. Storia della Puglia, Dal Seicento ad oggi. GLF Editori Laterza.

Milella, P., Bisantino, T., Gentile, F., Iacobellis, V., Trisorio Liuzzi, G., 2012. Diagnostic analysis of distributed input and parameter datasets in Mediterranean basin streamflow modeling. *Journal of Hydrology*, 472-473, 262-276.

Moriasi D., Arnold J., Van Liew M., Bingner R.L., Harmel R., Veith T., 2007. Modelevaluation guidelines for systematic quantification of accuracy in watershedsimulations. *Transactions of the ASABE* 50 (3), 885–900.

Nash, J.E., Sutcliffe, V., 1970. River flow forecasting through conceptual models I. Adiscussion of principles. *Journal of Hydrology* 10, 282–290.

Ott L., Larson R.F., Mendenhall W., 1983. Statistics: A Tool for the Social Sciences. Duxbury Press: Boston, MA.

Parajuli, P.B., Nelson, N.O., Frees, L.D., Mankin, K.R., 2009. Comparison of AnnAGNPSand SWAT model simulation results in USDA-CEAP agricultural watersheds insouth-central Kansas. *Hydrological Processes* 23, 748–763.

Pelacani S., Märker M., Rodolfi G., 2008. Simulation of soil erosion and deposition in a changing land use: A modelling approach to implement the support practice factor. *Geomorphology*, 99, 329-340.

Persichillo M. G., Bordoni M., Cavalli M., Crema S., Meisina C., 2017. The role of human activities on sediment connectivity of shallow landslides. *CATENA* 160, 261-274. doi: 10.1016/j.catena.2017.09.025

Petit C., Scudder T., Lambin E., 2001. Quantifying processes of land-cover change by remote sensing: resettlement and rapid land-cover change in southeastern Zambia. *Int J Remote Sens*, 22 (17), 3435-3456.

Pignatti S., 1995. Ecologia vegetale. UTET, Torino.

Polemio M., Casarano D., 2008. Climate change, drought and groundwater availability in southern Italy. In: Climate Change and Groundwater. Geological Society, London, Special Pubblication, 288, 39-51.

Polyakov, V., Fares, A., Kubo, D., Jacobi, J., Smith, C., 2007. Evaluation of a non-pointsource pollution model, AnnAGNPS, in a tropical watershed. *Environmental Modelling and Software* 22, 1617–1627.

Pontius R., Millones M., 2011. Death to Kappa: birth of quantity disagreement and allocation disagreement for accuracy assessment. *International Journal of Remote Sensing*. 32: 4407–4429.

Praskievicz S., Chang H., 2011. Impacts of climate change and urban development on water resources in the Tualatin River Basin, Oregon. *Ann Assoc Am Geogr*, 101 (2), 249–271.

Rawat J.S. and Kumar, 2015. Monitoring land use/cover change using remote sensing and GIS techniques: a case study of Hawalbagh block, district Almora, Uttarakhand, India. *The Egyptian Journal of Remote Sensing and Space Sciences*,18, 77-84.

Renard K.G., Foster G.R., Weesies G.A., McCool D.K., Yoder D.C., 1997. Predicting soil erosion by water: a guide to conservation planning with the revised universal soil loss equation (RUSLE). USDA Handbook No. 703. Department of Agriculture, Washington, DC, USA.

Romano G., Dal Sasso P., Trisorio Liuzzi G., Gentile F., 2015. Multi-criteria decision analysis for land suitability mapping in a rural area of Southern Italy. *Land Use Policy*, 48, 131-143.

Rounsevell M.D., Reginster I., Arujo M.B., Carter T.R., Dendoncker R., Ewert F., House J.I., Kankaanpää S., Leemans R., Metzger M.J., Schmit C., Smith P., Tuck G., 2006. A coherent set of future land use change scenarios for Europe. *Agriculture, Ecosystems and Environment*, 114, 57-68.

Saxton, K. E., & Rawls, W. J., 2006. Soil Water Characteristic Estimates by Texture and Organic Matter for Hydrologic Solutions. *Soil Sci. Soc. Am. J.*, 70(5), 1569-1578. doi: 10.2136/sssaj2005.0117.

SCS, 1986. Technical Release 55: Urban Hydrology for Small Watersheds. United States Department of Agriculture, Natural Resources Conservation Service, Conservation Engineering Division.

Sexton J.O., Urban D.L., Donohue M.J., Song C., 2013. Long-term land cover dynamics by multi-temporal classification across the Landsat-5 record. *Remote Sensing Of Environment*, 128, 246-258.

Shamshad, A., Leow, C. S., Ramlah, A., Wan Hussin, W. M. A., & Mohd. Sanusi, S. A., 2008. Applications of AnnAGNPS model for soil loss estimation and nutrient loading for Malaysian conditions. *International Journal of Applied Earth Observation and Geoinformation*, 10(3), 239-252. doi: http://dx.doi.org/10.1016/j.jag.2007.10.006.

Shrestha, S., Mukand, S., Babel, A., Das Gupta, F., 2006. Kazama evaluation of annualized agricultural non-point source model for a watershed in the Siwalik Hillsof Nepal. *Environmental Modelling and Software* 21, 961–975.

Shuttle Radar Topographic Mission (SRTM) – CGIAR Consortium for Spatial Information. http://srtm.csi.cgiar.org/SELECTION/inputCoord.asp (Accessed on 2016/05/18).

Taguas, E.V., Ayuso, J.L., Pe˜na, A., Yuan, Y., Pérez, R., 2009. Evaluating and modelling the hydrological and erosive behavior of an olive orchard micro-catchment under no-tillage with bare soil in Spain. *Earth Surface Processes and Landforms* 34 (5), 738–751.

Theobald D., Hobbs N., 2002. A framework for evaluating land use planning alternatives: protecting biodiversity on private land. *Conserv Ecol*, 6 (1), p. 5 http://www.consecol.org/vol6/iss1/art5

Theurer F.D., Clarke C.D., 1991. Wash load component for sediment yield modeling. Proc. 5th Federal Interagency Sedimentation Conf., March 18-21, Las Vegas, NV, USA, pp 7-1 to 7-8.

Theurer F.D., Cronshey R.G., 1998. AnnAGNPS - Reach routing processes. Proc. 1st Federal Interagency Hydrologic Modeling Conf., April 19-23, Las Vegas, NV, USA, 1-25 to 1-32.

Trombetta, A., Iacobellis, V., Tarantino, E., Gentile, F., 2016. Calibration of the AquaCrop model for winter wheat using MODIS LAI images. *Agricultural Water Management*, 164 (Part 2), 304-316.

Tu J., 2009. Combined impact of climate and land use changes on streamflow and water quality in eastern Massachusetts, USA. *J Hydrol*, 379, pp. 268–283.

USDA National Engineering Handbook, 1972. Hydrology Section 4. Soil Conservation Service, Washington, DC, Chapters 4–10, 16, 19.

USDA-ARS. 2006. AnnAGNPS - Annualized agricultural non-point source pollution model. Available from: http://www.ars.usda.gov/Research/docs.htm?docid=5199 Accessed: November 2011.

Verburg P.H., Shot P.P., Dijst M.J., Veldkamp A., 2004. Land use change modelling: Current practices and research priorities. *GeoJournal*, 61, 309-324.

Wang X., Zhao X., Zhang Z., Yi L., Zuo L., Wen Q., Liu F., Xu J., Hu S., Liu B., 2016. Assessment of soil erosion change and its relationships with land use/cover change in China from the end of the 1980s to 2010. *Catena*, 137, 256-268.

White M.D., Greer K.A., 2006. The effects of watershed urbanization on the stream hydrology and riparian vegetation of Los Peñasquitos Greek, California. *Landscape and Urban Planning*, 74, 125–138.

Wilson C.O., Weng Q., 2011. Simulating the impacts of future land use and climate changes on surface water quality in the Des Plaines River watershed, Chicago Metropolitan Statistical Area, Illinois. *Science of the Total Environment*, 409, 4387-4405.

Wu Q., Li H., Wang R., Paulussen J., He Y., Wang M., Wang B., Wang Z., 2006. Monitoring and predicting land use change in Beijing using remote sensing and GIS. *Landscape Urban Plann*, 78, 322–333.

Yuan Y., Bingner R.L., Rebich R.A., 2001. Evaluation of AnnAGNPS on Mississippi Delta MSEA watersheds. *Transactions of the American Society of Agricultural Engineers* 44 (5), 1183–1190.

Yuan Y., Bingner R.L., Theurer F., 2006. Subsurface flow component for AnnAGNPS. *Trans. ASAE* 22:231-41.

Young R.A., Onstad C.A., Bossch D.D., Anderson W.P., 1989. AGNPS: a non-point source pollution model for evaluating agricultural watersheds. *Journal of Soil and Water Conservation*, 44 (2), 168–173.